Available online at www.sciencedirect.com

SCIENCE DIRECT®

Developmental Biology 280 (2005) 133–149

DEVELOPMENTAL BIOLOGY

www.elsevier.com/locate/ydbio

Cooperative function of *deltaC* and *her7* in anterior segment formation

Andrew C. Oates[a,*], Claudia Mueller[a], Robert K. Ho[b]

[a]*Max Planck Institute of Molecular Cell Biology and Genetics, Pfotenhauerstrasse 108, 01307 Dresden, Germany*
[b]*Department of Organismal Biology and Anatomy, University of Chicago, Chicago, IL 60637, USA*

Received for publication 31 March 2004, revised 12 January 2005, accepted 12 January 2005

Abstract

Segmentation of paraxial mesoderm in vertebrates is regulated by a genetic oscillator that manifests as a series of wavelike or cyclic gene expression domains in the embryo. In zebrafish, this oscillator involves members of the Delta/Notch intercellular signaling pathway, and its down-stream targets, the *Her* family of transcriptional repressors. Loss of function of any one of the genes of this system, such as *her7*, gives rise to segmentation defects in the posterior trunk and tail, concomitant with a disruption of cyclic expression domains, indicating that the oscillator is required for posterior segmentation. Control of segmentation in the anterior trunk, and its relationship to that of the posterior is, however, not yet well understood.

A combined loss of the cyclic *Her* genes *her1* and *her7* disrupts segmentation of both anterior and posterior paraxial mesoderm, indicating that *her* genes function redundantly in anterior segmentation. To test whether this anterior redundancy is specific to the *her* gene family, or alternatively is a more global feature of the segmentation oscillator, we looked at anterior segmentation after morpholino knock down of the cyclic cell-surface Notch ligand *deltaC* (*dlc*), either alone or in combination with *her7*, or other Delta/Notch pathway genes. We find that *dlc* is required for coherence of wavelike expression domains of cyclic genes *her1* and *her7* and maintenance of their expression levels, as well as for cyclic transcription of *dlc* itself, confirming that *dlc* is a component of the segmentation oscillator. Dose dependent, posteriorly-restricted segmentation defects were seen in the *dlc* knock down, and in combination with the *deltaD* or *notch1a* mutants. However, combined reduction of function of *dlc* and *her7* results in defective segmentation of both anterior and posterior paraxial mesoderm, and a failure of cyclic expression domains to initiate, similar to loss of both *her* genes. Thus, anterior segmentation requires the functions of both *her* and *delta* family members in a parallel manner, suggesting that the segmentation oscillator operates in paraxial mesoderm along the entire vertebrate axis.

Keywords: *deltaC*; *her7*; *beamter*; *after eight*; *deadly seven*; *deltaD*; Segmentation; Somitogenesis; Oscillator; Notch signaling; Somites

Introduction

The segmented architecture of the vertebrate embryo and its relationship to segmented structures of the adult have been appreciated for centuries, but the mechanisms whereby this spatial pattern emerges during embryogenesis are only just being deciphered. In all vertebrates, the paraxial mesoderm, which later gives rise to the reiterated skeletal elements and muscles of the adult body, segments through serial formation of blocks of cells called somites from the morphologically unpatterned Pre-Somitic Mesoderm (PSM). A remarkable insight into this process has come from findings in chick, mouse, and zebrafish embryos of dynamic, wavelike gene expression patterns in the PSM (reviewed in Pourquie, 2001; Rida et al., 2004). These expression domains initiate in the posterior PSM with a period equal to the time interval between somite formation, travel anteriorly through the PSM from the tailbud, then arrest at a location in the anterior PSM that predicts the site of future somite boundary formation. The mRNAs and proteins with such expression patterns, products of the so-called cyclic genes, do not themselves propagate through the PSM, nor do cells of the PSM move with similar velocity (Palmeirim et al., 1997). Rather, these cyclic

* Corresponding author.
E-mail address: oates@mpi-cbg.de (A.C. Oates).

0012-1606/$ - see front matter © 2005 Elsevier Inc. All rights reserved.
doi:10.1016/j.ydbio.2005.01.010

expression patterns are thought to represent the coordinated activity of genetic oscillators in each cell in the PSM. Indeed, studies of cyclic *Hes1* gene mRNA and protein oscillations in cultured mouse cells suggest that for several cycles this phenomenon can be maintained in a cell-autonomous manner (Hirata et al., 2002). At present, cyclic expression patterns in the PSM are the only measurement of segmentation oscillator integrity in the embryo. The role of this oscillator in segmentation and its composition and underlying mechanism are the subjects of continuing study.

To date, the cyclic genes (with the exception of *axin2*; Aulehla et al., 2003) are members of the canonical Delta/Notch signal transduction system: either ligands (*deltaC* (Jiang et al., 2000)), modifiers of Notch receptor glycosylation (*Lfng* (Aulehla and Johnson, 1999; McGrew et al., 1998)), or target genes of the activated Notch receptor such as members of the Hairy-Enhancer of Split Related (HER) family of transcriptional repressors (*c-hairy1*, *c-hairy2*, *Hes1*, *Hes7*, *Hey2*, *her1*, *her7*, and *esr9* (Bessho et al., 2001a; Henry et al., 2002; Holley et al., 2000; Jouve et al., 2000; Leimeister et al., 2000; Li et al., 2003; Oates and Ho, 2002; Palmeirim et al., 1997; Sawada et al., 2000)). Furthermore, cyclic gene transcription of *Lfng* in the mouse is dependent on Notch-responsive elements in the *Lfng* promoter (Cole et al., 2002; Morales et al., 2002). This raises the possibility that the action of this signaling system is linked to or even constitutes a part of the oscillatory mechanism.

Loss of cyclic gene function, such as for *Lunatic fringe* (*Lfng*) or *Hes7* in mouse (Bessho et al., 2001b, 2003; Evrard et al., 1998; Zhang and Gridley, 1998), and *deltaC*, *her1*, *her7* in zebrafish (Henry et al., 2002; Holley et al., 2002; Oates and Ho, 2002), results in a segmentation phenotype characterized by irregularly shaped, partial, and bilaterally asymmetric furrow formation. The combined loss of *her1* and *her7* results in the most severe segmental defects in zebrafish, but sclerotome precursors, twitching muscle, and epithelial furrows are nevertheless generated from the paraxial mesoderm (Oates and Ho, 2002), indicating that cyclic gene function and, by inference, the oscillator, is required for, and restricted to, the positioning of the segmental boundaries only.

By definition (Palmeirim et al., 1997), a *component* of the segmentation oscillator is required for some aspect of oscillator integrity, whereas an *output* is a means of translating the periodicity of the oscillator into an effect in the embryo that does not feed back into the oscillatory mechanism. In operational terms, the loss of a component's function would be expected to disrupt the wavelike expression domains of cyclic genes, but the loss of an output would not, although it may nevertheless result in somitogenic defects. Using these criteria, the cyclic *her7*, *her1*, and *Hes7* genes of zebrafish and mouse are components of the oscillator (Bessho et al., 2001b, 2003; Henry et al., 2002; Holley et al., 2002; Oates and Ho, 2002), whereas the *Hes1* gene of mice appears to be an output (Ishibashi et al., 1995; Jensen et al., 2000; Jouve et al., 2000). Removing either *her7* or both *her7* and *her1* function in zebrafish results in a loss of coordinated oscillatory expression of the cyclic genes; instead, they are expressed evenly throughout the PSM (Gajewski et al., 2003; Henry et al., 2002; Oates and Ho, 2002). Similarly, loss of *Hes7* in the mouse results in the loss of coordinated oscillations and widespread expression of *Lfng* (Bessho et al., 2001b, 2003; Hirata et al., 2004), suggesting that the *HER* genes together normally function in a repressive capacity within the oscillator. Indeed, mathematical modeling of a *Her*-driven negative feedback loop suggests that this interaction, combined with adequate delay, is sufficient for oscillation (Lewis, 2003), although recent data suggest that *her1* may also be capable of acting as an activator in the non-cyclic anterior PSM (Gajewski et al., 2003).

Loss of function of several non-cyclic members of the Delta/Notch signaling system also gives rise to somitogenic defects during mouse and zebrafish embryogenesis, including lesions in *deltaD*, *Dll1*, *Dll3*, *mind bomb*, *notch1a*, *Notch1*, *Presenilin1*, and *Su(H)* (Conlon et al., 1995; Holley et al., 2000, 2002; Hrabe de Angelis et al., 1997; Itoh et al., 2003; Koizumi et al., 2001; Kusumi et al., 1998; Oka et al., 1995; Sieger et al., 2003). Although their mRNAs do not cycle in the PSM, it is possible that one or more properties of their proteins, such as post-translational modification, or the embryonic or sub-cellular distribution, may possess periodic character. Importantly, mutations in the *deltaD*, *Dll1*, *Dll3*, *notch1a*, and *Su(H)* genes result in perturbation of cyclic gene expression (Barrantes et al., 1999; Dunwoodie et al., 2002; Holley et al., 2000, 2002; Jouve et al., 2000; Morales et al., 2002; Sieger et al., 2003), suggesting that they may also be thought of as components of the oscillator.

Loss of function of both cyclic and non-cyclic Delta/Notch and *Her* genes preferentially affects segmentation in the more posterior parts of the animal. In principle, this may be the result of independent mechanisms regulating anterior and posterior trunk segmentation. Alternatively, there may be a single mechanism operating along the A/P axis that requires multiple lesions to be inactivated due to component redundancy. In zebrafish embryos, the onset of defective somitogenesis is sudden, and the position along the A/P axis where the first defective segment occurs, known as the Anterior Limit of Defects (ALD; Oates and Ho, 2002), is characteristic for each mutant or morpholino-induced phenotype. Examination of the wavelike expression domains in these different mutant and morpholino-injected embryos reveals an important relationship between the coherence of cyclic expression patterns and ALD: cyclic patterns are initially normal in the PSM, but gradually lose coherence and at the position of the ALD, have lost any sign of wavelike organization (Jiang et al., 2000; Oates and Ho, 2002).

When combined with a reduction in function of the cyclic *her7* gene, the Delta/Notch loss-of-function mutants *after eight/deltaD* and *deadly seven/notch1a* show a rostral shift in ALD (Oates and Ho, 2002), indicating that these

genes have redundant functions in the segmentation of the trunk anterior to their single gene ALD. However, none of these combinations, nor double mutants between *after eight/deltaD*, *deadly seven/notch1a*, or *beamter* (van Eeden et al., 1996), nor a knock down of the Notch transcriptional effector *Su(H)* (Sieger et al., 2003) has been reported to affect the anterior-most five or six segments. In contrast, combined *her1* and *her7* reduction-of-function generates a more severe somitogenic phenotype, shifting the ALD to the very anterior end of the paraxial mesoderm (Henry et al., 2002; Oates and Ho, 2002), and in this extreme case, there is no evidence of cyclic expression domains at any stage (Oates and Ho, 2002), again correlating ALD and loss of cyclic coherence. We also previously showed that injection of *her7* morpholino into the *beamter* mutant background produced similar defects in anterior and posterior segmentation (Oates and Ho, 2002), but without the molecular identity of *beamter*, further conclusions were not possible (see Discussion). These results raise the possibility that the anterior segments do not require Delta/Notch signaling to form and rely instead on the *Her* genes, potentially interacting in the anterior with other signaling pathways.

In this report, we directly test this proposition by generating a combined reduction in function for *her7* and the cyclic Notch ligand *deltaC* and analyzing the formation of the anterior segments. Zebrafish *deltaC* (*dlc*) is the only known gene of the Delta family from any species to exhibit cyclic expression patterns (Jiang et al., 2000), but whether these oscillations are transcriptionally controlled, like those of the *her1* (Gajewski et al., 2003), *Hes7* (Hirata et al., 2004), and *Lfng* gene (Cole et al., 2002; Morales et al., 2002), is unknown. We show here that cyclic *dlc* expression patterns can be seen in prespliced mRNA, indicating that the pattern is generated by cyclic transcription. The effects of *dlc*-targeted morpholinos on cyclic expression domain coherence during development, and on transcription from the *dlc* genomic locus indicate that *dlc* is a component of the oscillator, consistent with the original conclusions of Holley et al. (2002), and show that *dlc* has a role in activating all the known cyclic genes, in contrast to the inhibitory effect of the *her* genes on cyclic expression. We find that a reduction of *dlc* function causes posterior somite defects resembling the known Delta/Notch pathway mutants and the *her7* morpholino-induced phenotype, whereas molecular segment polarity defects differ from those seen in the case of *her7*-morpholino and *aei/deltaD* mutant phenotypes. Although combined loss of *dlc* with other components of the oscillator does not generate large rostral shifts in ALD, reducing both *her7* and *dlc* function produces profound segmental defects from the very anterior of the paraxial mesoderm. This effect is similar to the combined *her7* and *her1* reduction-of-function phenotype, indicating that *dlc* has a redundant role in anterior segmentation.

Materials and methods

Fish care and mutant stocks

Zebrafish was raised according to standard methods and embryos derived from natural spawning were staged according to (Kimmel et al., 1995). Alleles of mutant strains *after eight* (aei^{tr233}), *deadly seven* (des^{tp37}), and *beamter* (bea^{tm98}) were previously described (van Eeden et al., 1996).

Morpholino design and injection

Morpholino antisense oligonucleotides (Nasevicius and Ekker, 2000) were designed to 5′ regions of the cDNAs of *her7* and *dlc* and synthesized by Gene-tools LLC (Pilometh, Oregon). To avoid confusion between different morpholinos targeted to the same genes, we have renamed some of our previously used morpholinos to reflect a growing convention and to acknowledge other morpholinos that were published while a previous manuscript was in press. The her7m1 (now her7MO1) her7m2 (now her7MO2) morpholinos have been used previously (Oates and Ho, 2002), whereas dlcMO3 and dlcMO4 are described here for the first time: dlcMO3 GAGCCATCTTTGCCTTCTTGTCTGC, dlcMO4 CTACTGAACGATAGCAGACTGTGAG. Note that dlcMO3 almost entirely overlaps dlcmo1 (Holley et al., 2002). Morpholino or morpholino combinations were titrated over a concentration series from 0.2 ng/nL to 6 ng/nL as recorded in Tables 1 and 2. The upper limit of these series was reached when embryos first exhibited necrosis under the head, which was often accompanied by curvature of the axis, both phenotypes being attributable to non-specific effects due to morpholino toxicity (Ekker and Larson, 2001).

In situ hybridization, riboprobe generation, and image acquisition

In situ hybridization was as previously described (Oates and Ho, 2002), using riboprobes to *her7*, *mespa*, *mespb* and *deltaC* (Oates and Ho, 2002), *myoD* (Weinberg et al., 1996), *paraxial protocadherin* (Yamamoto et al., 1998), *deltaD* (Dornseifer et al., 1997), *her1* (Muller et al., 1996), *notch1a*, *notch5* (Westin and Lardelli, 1997), with additional riboprobes *notch6* (Westin and Lardelli, 1997), *ephA4*, *ephrinB2* (Durbin et al., 1998). Template for *fgfr4* riboprobe (Thisse et al., 1995) was amplified from cDNA using nested PCR with external primers: fgfr4-1 tgaccagctgtctctcacactca and fgfr4-4R ctgacattcacaagatgtgcca, and internal primers: fgfr4-2 atgttgagcatcttaaaggt and fgfr4-3R ctatcgcattgtcgtctttaggt. The probe we previously described as *twitchin* has been entered into the database by Y-L Yan and JH Postlethwaite (University of Oregon) as a *titin* homolog with accession number: AY081167. Template for a 351 bp *dlc* intron-derived riboprobe was amplified from genomic DNA based on sequence from the zebrafish genome project (Sanger Centre, accession number:

Table 1
Incidence and severity of segmental defects in zebrafish embryos injected with *dlc*-targeted morpholinos

Treatment	Conc. (ng/nL)	*n*	Segmental phenotype at 26 hpf[a]				Total with segmental defects (%)
			Normal	Register	Boundary	Register and boundary	
*dlc*MO3	0.5	51	51 (100)	0	0	0	0
	1	20	10 (50)	0	3 (15)	7 (35)	10 (50)
	2	18	3 (17)	0	1 (5)	14 (78)	15 (83)
*dlc*MO4	1	52	52 (100)	0	0	0	0
	3	23	19 (83)	0	0	4 (17)	4 (17)
	5	29	18 (62)	0	6 (20)	5 (17)	11 (38)
	7	41	21 (51)	0	9 (22)	11 (27)	20 (49)
*dlc*MO3 + MO4	0.2 + 0.2	62	25 (40)	0	0	37 (60)	37 (60)
	0.5 + 0.5	79	10 (23)	0	0	69 (87)	69 (87)
	1 + 1	74	7 (9)	0	1 (1)	64 (86)	65 (88)
	1 + 2	67	1 (1)	0	0	66 (99)	66 (99)
	1 + 3	42	1 (2)	1 (2)	0	40 (95)	41 (98)
	1 + 6	37	1 (3)	0	0	36 (97)	37 (97)

[a] Segmental phenotype was assayed by the shape of the transverse myosepta at 26 hpf revealed by *titin* in situ hybridyzation. A register defect was the loss of bilateral symmetry across the midline of otherwise normally shaped myotomes. A boundary defect was the aberrant formation of a transverse myoseptum either bifurcated, partial, or twisted in shape. A register and boundary defect was scored when asymmetrical, aberrant myosepta were present in a contiguous region along the axis.

zC244M22) using primers directed to the ends of intron 4: dlcIn1 cgtaagtgtttatgaatagcca and dlcIn2R tggctgtttagaaaggataggga. Hybridization and high temperature washing of the *dlc* intronic riboprobe were carried out at 60°C. Fluorescent visualization of transcript accumulation marked by Fast Red substrate (Roche, NY) was recorded on a Zeiss LSM 405 confocal microscope (Zeiss, NY) using standard settings for rhodamine detection. For each of the experiments in (Figs. 3, 4 and 6), all color development for a given probe was done strictly in parallel to enable comparisons between panels within a figure.

Results

Over-expression of *dlc* mRNA in zebrafish was reported to disrupt somitogenesis in the paraxial mesoderm without affecting the striped pattern of *her1* expression in the PSM, suggesting that its function is restricted to the refinement of boundaries in the anterior PSM (Takke and Campos-Ortega, 1999). This result is therefore consistent with a role for *dlc* as an output of the oscillator. In a separate study, morpholino-induced reduction of *dlc* function was found to cause a disruption of cyclic *her1* and *dlc* expression, implying that *dlc* is in fact a component of the oscillator (Holley et al., 2002). Somitogenic defects were seen along the entire body axis (Holley et al., 2002), in contrast to the posterior-specific loss-of-function phenotypes of all other previously described Delta/Notch signaling components. Before assessing the interaction between *dlc* and *her7* in somitogenesis, we sought to clarify the nature of the *dlc* knock down phenotype.

Reduction of deltaC function causes segmental abnormalities in the posterior trunk and tail

To determine the requirement for *deltaC* (*dlc*) function in segmentation, we designed antisense morpholinos (MOs) targeted to the 5′ UTR region of the *dlc* mRNA, injected them into early zebrafish embryos, and assayed the formation of the myotome boundaries of the trunk using the expression of the zebrafish *titin* gene at 26 h post fertilization (hpf) as a marker. Introduction of either *dlc*MO3 or *dlc*MO4 individually resulted in a segmental phenotype in the posterior trunk that was weakly penetrant even at the highest doses of MO that gave otherwise normally formed embryos (Table 1 and data not shown). Since others have reported targeting synergism upon injection of multiple MOs directed to different regions of the same mRNA (Cui et al., 2001; Ekker

Table 2
Incidence and severity of segmental defects in zebrafish embryos co-injected with two *her7*-targeted morpholinos

Treatment	Conc. (ng/nL)	*n*	Segmental phenotype at 26 hpf[a]				Total with segmental defects (%)
			Normal	Boundary	Register	Boundary and register	
*her7*MO1 + MO2	0.5 + 0.5	48	11 (23)	0	1 (2)	36 (75)	37 (77)
	1 + 1	63	4 (6)	2 (3)	2 (3)	53 (84)	57 (90)
	2 + 2	100	1 (1)	0	0	99 (99)	99 (99)
	3 + 3	88	3 (3)	0	0	85 (97)	85 (97)

[a] See legend to Table 1.

and Larson, 2001), we assayed the effect of co-injection of *dlc*MO3 and *dlc*MO4. We observed a highly penetrant segmental phenotype in the posterior trunk and tail involving both register and boundary defects (Oates and Ho, 2002) (Table 1 and Figs. 1A–D). These defects are very similar in appearance to those resulting from reduction of *her7* function (Henry et al., 2002; Oates and Ho, 2002) and those observed in the Delta/Notch signaling mutants *after eight/deltaD* (*aei/dld*), *deadly seven/notch1a* (*des/n1a*), and *beamter* (*bea*) (Oates and Ho, 2002; van Eeden et al., 1996), suggesting that a similar process has been perturbed. Titration of the combined *dlc*MO dose revealed an ALD that shifted rostrally with higher concentrations, but stabilized at segment 5 (Fig. 1E), indicating a preferential requirement for *dlc* function in the formation of segments of the posterior trunk and tail. These results are in contrast to those of Holley et al. (2002), where segmentation defects were seen throughout the axis (see Discussion).

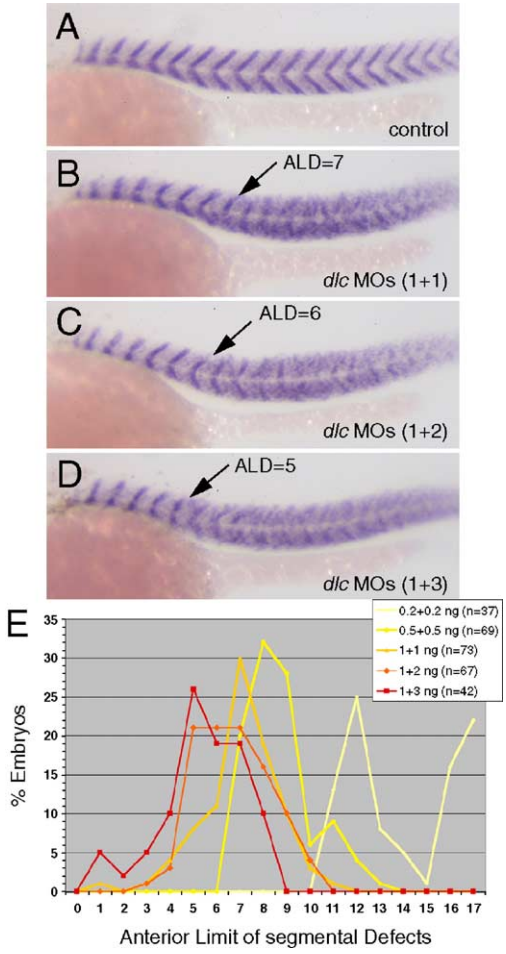

Fig. 1. Effect of reduction of *deltaC* function on zebrafish segmentation. (A–D) Myotome boundaries of the trunk marked by *titin* expression are shown in 26 hpf embryos in lateral view with anterior to the left and dorsal upwards. Arrows in panels (B–D) indicate Anterior Limit of Defects (ALD) in each embryo. (A) Uninjected control. Representative embryos injected with 1 ng/nL (B), with 1 and 2 ng/nL (C) and with 1 and 3 ng/nL (D) of each of the morpholinos *dlc*MO3 and *dlc*MO4, respectively. (E) Data from a histogram (plotted as line graph) showing the distribution of ALD for populations of embryos injected with increasing concentrations of combined morpholinos, indicating a final ALD at segment 5. Embryos injected with doses higher than 1 + 3 ng/nL of the combined morpholinos exhibited necrosis and non-specific defects and were not included.

Loss of segment polarity in the PSM

To investigate the underlying cause of these segmental abnormalities, we examined morphology and marker gene expression during early stages of somitogenesis. Embryos injected with *dlc*MOs generated well-formed anterior trunk somites, but their posterior trunk somite furrows were abnormally spaced and oriented (data not shown), indicating that the segmental abnormalities observed at 26 hpf arose during somitogenesis. At the 10 somite stage, examination of markers of caudal and rostral half-segment identity in the PSM, such as the caudally-expressed *myoD* (29/30; Fig. 2A) and *fgfr4* (9/10; Fig. 2C) and the rostrally-expressed *fgf8* and *mespb* (15/15, 14/14, Figs. 2B,F), revealed a loss of the normal striped pattern, indicating that segment polarity had been disrupted in the PSM.

Expression of *notch5* and *mespa* was essentially abolished in the PSM of *dlc*MO-treated embryos at 10 somites (25/25, 31/31; Figs. 2Eb,Gb). Importantly, these results differ from those due to reduction of *her7* function, where despite disruption of segmental patterning, *notch5* (12/12) and *mespa* (17/17) expression levels are normal (Figs. 2Ec,Gc and Oates and Ho, 2002), and from the combined *her1* and *her7* phenotype, where *notch5* and *mespa* expression is only slightly reduced (Henry et al., 2002; Oates and Ho, 2002). Expression of *notch5* in *aei/dld* mutant embryos was also down-regulated in the paraxial mesoderm, but in contrast to *dlc*MO-injected embryos, a diffuse band of expression persisted in the anterior PSM (18/18; bracket, Fig. 2Ed). In contrast, the levels of *notch6* expression were not significantly changed over wild type in the PSM of *dlc*MO-injected embryos (Fig. 2D). Loss of *mespa* expression is also seen in *aei/dld* and other Delta/Notch mutants (18/18; Fig. 2Gd and data not shown; Durbin et al., 2000; Sawada et al., 2000). Indeed, examination of *mespa* expression at the 1 somite stage after *dlc*MO injection revealed that the *mespa* anterior PSM domain is never formed in these embryos (data not shown). These results suggest that, in addition to a spatial patterning role, *dlc* may be directly required for expression of a subset of the segment polarity genes.

The delay and disorganization of the morphological furrows in the paraxial mesoderm of *dlc*MO-injected embryos were investigated through the expression of genes known to play a role in this process. The cell adhesion molecule *paraxial protocadherin* (*papc*) and the contact repulsion receptors *ephA4* and *ephrinB2* have been shown to play roles in generating the epithelial boundaries of the forming somites in mice, *Xenopus*, and zebrafish (Durbin et al., 1998, 2000; Kim et al., 2000; Rhee et al., 2003; Yamamoto et al., 1998). In *dlc*MO-

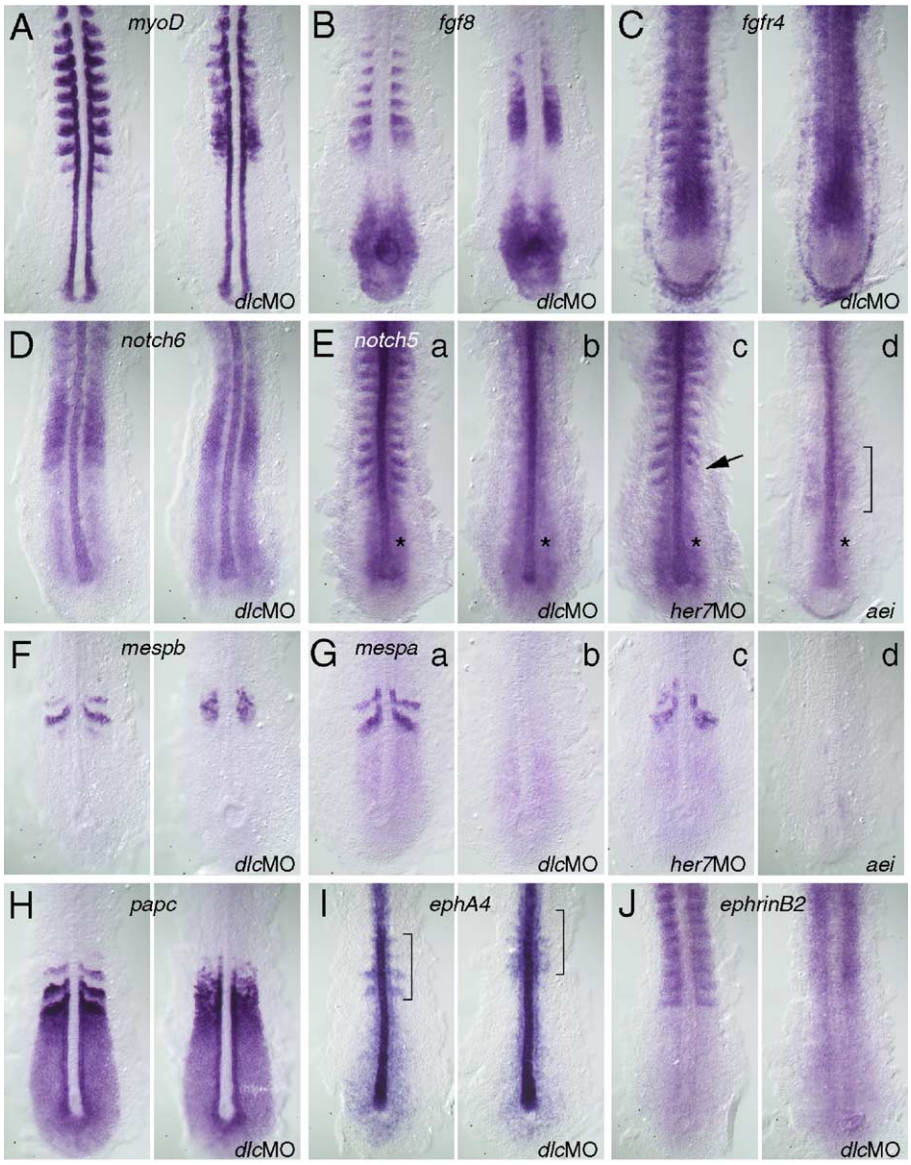

Fig. 2. Effect of reduction of *deltaC* function on somitogenesis and segment polarity. Gene expression patterns in PSM and trunk somites of embryos at 14 hpf (10 somites) are shown in dorsal view after flat mounting with anterior upwards. In each pair of panels (A–D, F, H–J), an uninjected control is on the left and an embryo coinjected with 1 ng/nL *dlc*MO3 and 2 ng/nL *dlc*MO4 is on the right. In panels (E) and (G), the uninjected embryo is on the left (a) and embryos injected with *dlc*MOs (b), *her*7MOs (c; 2 ng/nL *her*7MO1 and 2 ng/nL *her*7MO2), or homozygous for the *aei/dld* mutation (d) are ordered to the right. Expression of *myoD* (A), *fgf8* (B), *fgfr4* (C), *notch6* (D), *notch5* (E), *mespb* (F), *mespa* (G), *papc* (H), *ephA4* (I), and *ephrinB2* (J) is shown. Brackets in panels (Ed) and (I) and arrow in panel (Ec) indicate affected regions, asterisks in panel (E) mark expression in overlying neural plate.

injected embryos at 10 somites, expression of *papc*, *ephA4*, and *ephrinB2* was abnormal in the PSM and somitic regions (10/11; 9/9; 8/8; Figs. 2H–J) showing a disruption of the normal striped organization. In addition, the posterior extent of the *ephA4* expression domain was shifted rostrally by two segments (bracket), corresponding to a developmental delay of 1 h, although we cannot exclude that *ephA4*, which is a very weak probe in the PSM, may instead be expressed at lower levels, giving the impression of a delay. Combined, these findings indicate that normal *dlc* function is also required for the correct timing and spatial organization of the expression of genes responsible for the morphological events of somitogenesis. Thus, the morphological defects present at 26 hpf are preceded during somitogenesis by severe defects in segment polarity.

Gradual loss of her gene wavelike expression domains precedes morphological defects

The loss of the dynamic wavelike expression patterns of the cyclic genes in embryos with reduction of *her7* function indicates that *her7* is a component of the segmentation oscillator (Oates and Ho, 2002). To determine whether the cyclic *dlc* gene is also a component of the segmentation oscillator, we examined the expression of

the other cyclic genes *her1* and *her7* in a time series of embryos injected with *dlc*MOs at a concentration sufficient to produce an ALD of 7 (see Fig. 1). Embryos injected with *dlc*MOs retained wavelike expression domains of *her1* (n = 101) and *her7* (n = 77) up to bud stage, although these were predominantly diffuse and their level of expression was reduced in comparison to control embryos (asterisks, Figs. 3A,B,E,F,I,J,M,N. Note that, in panel N, the level of *her7* expression is difficult to visualize in whole-mounted embryos). By the 3 somite stage, *her1* expression was sharply reduced (n = 51), and expression of *her7* was almost undetectable in the PSM (n = 45), although still weakly present in the posterior tailbud (Figs. 3C,G,K,O), and this trend continued through the 5 somite stage (*her1* n = 59, *her7* n = 33; data not shown). Nevertheless, different patterns of the disorganized stripes could be seen from embryo to embryo within a clutch, suggesting that some residual cyclic organization remained (e.g. asterisks, Fig. 3G). However, by the 7 somite stage, *her1* was diffusely expressed throughout the anterior two-thirds of the PSM without evidence of wavelike expression domains (brackets; n = 20, Figs. 3D,H), and *her7* was expressed in the tailbud, the posterior one-third (brackets), and in a few scattered cells of the anterior-most PSM (asterisks) (n = 15, Figs. 3L,P), again without any organization into cyclic domains. The timing of the complete breakdown in wavelike expression domains correlates well with the observed ALD for this concentration of morpholinos at segment 7.

We also assayed the effect of *dlc* reduction of function on expression of the *aei/dld* and *des/n1a* genes, both of which are required for wavelike expression domain coherence (Holley et al., 2000, 2002; Jiang et al., 2000; Oates and Ho, 2002; van Eeden et al., 1998) and can thus be considered as non-cyclic components of the segmentation oscillator. Expression of *aei/dld* is variable in PSM of normal embryos (Fig. 3Q), but loses all variability and evidence of striped pattern after *dlc*MO injection (n = 15, Fig. 3R). In contrast to the cyclic *her* genes, the level of *aei/dld* mRNA is not appreciably lowered by *dlc*MOs (Figs. 3Q,R), nor is the level of *des/n1a* affected (n = 11, Figs. 3S,T), indicating that their mRNA expression levels are independent of *dlc* function. Thus, these results suggest that *dlc* is acting as a component of the segmentation oscillator, and not simply as an output. The severe reduction of expression levels of *her1* and *her7* is reminiscent of the effects on *her7* expression seen in *aei/dld*, *des/n1a*, and *bea* mutants, but contrasts with the elevation of cyclic gene expression seen after reduction of *her7* or *her1* and *her7* function (Oates and Ho, 2002), suggesting that part of the normal function of *dlc* is to maintain elevated expression of the cyclic genes.

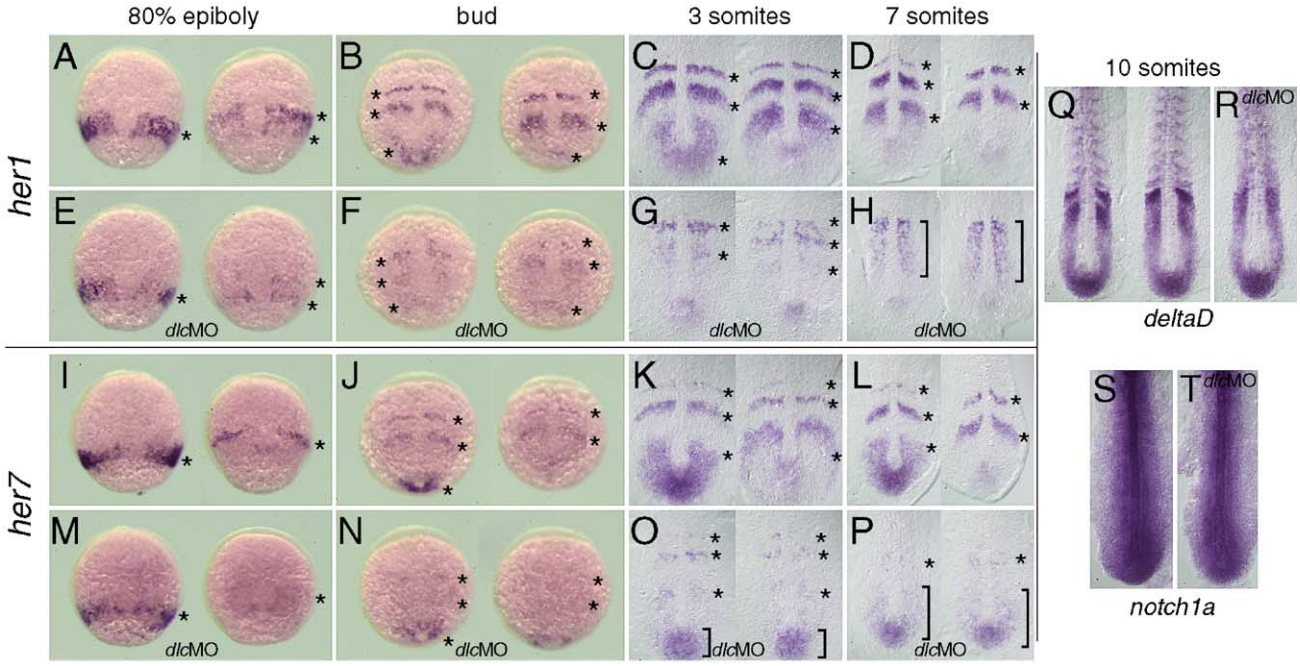

Fig. 3. Expression of the cyclic *her* genes in response to reduction of *deltaC* function. Expression in PSM of zebrafish cyclic genes *her1* (A–H) and *her7* (I–P) shown from 9 hpf (80% epiboly) to 13 hpf (7 somites). Expression of non-cyclic *deltaD* (*dld*; Q, R) and *notch1a* (S, T) shown at 14 hpf (10 somites). Embryos are displayed in whole mount (A, B, E, F, I, J, M, N) and in flat mount (C, D, G, H, K, L, O, P, Q–T) with (E–H, M–P, R, T) and without (A–D, I–L, Q, S) injection of 1 ng/nL *dlc*MO3 and *dlc*MO4. In each panel (A–D, I–L), two wild type embryos with representative phases of cyclic gene expression patterns are shown; wavelike expression domains are marked with asterisks. Batches of *dlc*MO-injected embryos show similar variability to wild type embryos at earlier stages (E, M), but at later stages, embryos in a batch are indistinguishable (H, P). Regions of invariant gene expression are denoted with brackets in panels (O), (H), and (P) and asterisks in panel (P). Note also that, across this time period, the level of transcript decreases in *dlc*MO-injected embryos. (Q, R) The effect of *dlc*MOs (as above) on the expression of *deltaD* showing a loss of patterning in the presence of normal levels of *dld* expression. (S, T) Expression levels of *notch1a* are not perturbed by injection of *dlc*MOs.

Cyclic expression of deltaC is transcriptionally controlled

Before examining the expression of *dlc* in *dlc*MO-injected embryos, we first addressed the origin of the cyclic *dlc* expression stripes. Transcriptional control of cyclic expression has been demonstrated for genes of the *Her* family in zebrafish and mouse (Gajewski et al., 2003; Hirata et al., 2004) and Lfng in chick (Morales et al., 2002) using intron-specific riboprobes. We therefore investigated the patterns of transcriptional activity directly from the *dlc* locus using a riboprobe derived from the fourth intron of the *dlc* gene. In wild type embryos of various developmental stages, a series of stripes were detected in the PSM (Figs. 4A,B), closely recapitulating those seen with a cDNA-derived (exonic) probe (Fig. 4C, Jiang et al., 2000). These stripes were notably less broad than the corresponding exonic signal, even after prolonged development, suggesting that only a subset of those cells highlighted by the exonic riboprobe was transcriptionally active at the *dlc* gene. We looked for confirmation of this scenario in the sub-cellular localization of signals from the cDNA-derived riboprobe.

Confocal microscopy of embryos hybridized with exonic *dlc* riboprobe revealed a difference in the localization of signal across the R/C axis of wavelike expression domains in the posterior and mid-PSM (Fig. 4D). At the rostral edge, a punctate signal was detected (domain b, arrows in right hand panel); more posterior to this was nuclear staining, and more posterior still, a diffuse cellular signal was evident (asterisks). Similar puncta have been observed using an intron-derived riboprobe to the chick *Lfng* gene (Morales et al., 2002) and likely correspond to the *dlc* locus. In addition, we observed that the *dlc* stripes in the anterior PSM were constituted largely from evenly distributed cellular staining (Fig. 4Da) whereas the posterior PSM *dlc* expression domains possessed a large proportion of punctate and nuclear signal (Fig. 4Dc). The thinner stripes seen with the intron probe likely represent the rostral portion of the stripe as defined by the exon probe. These results indicate that *dlc* expression, like cyclic genes from the *Her* and *Lfng* families, are driven by oscillating transcriptional activity.

Expression of deltaC is affected by reduction of deltaC function

To determine the effect of reduced *dlc* protein on its own gene expression patterns and RNA levels, we first examined *dlc* mRNA, as measured with a cDNA (exonic) riboprobe,

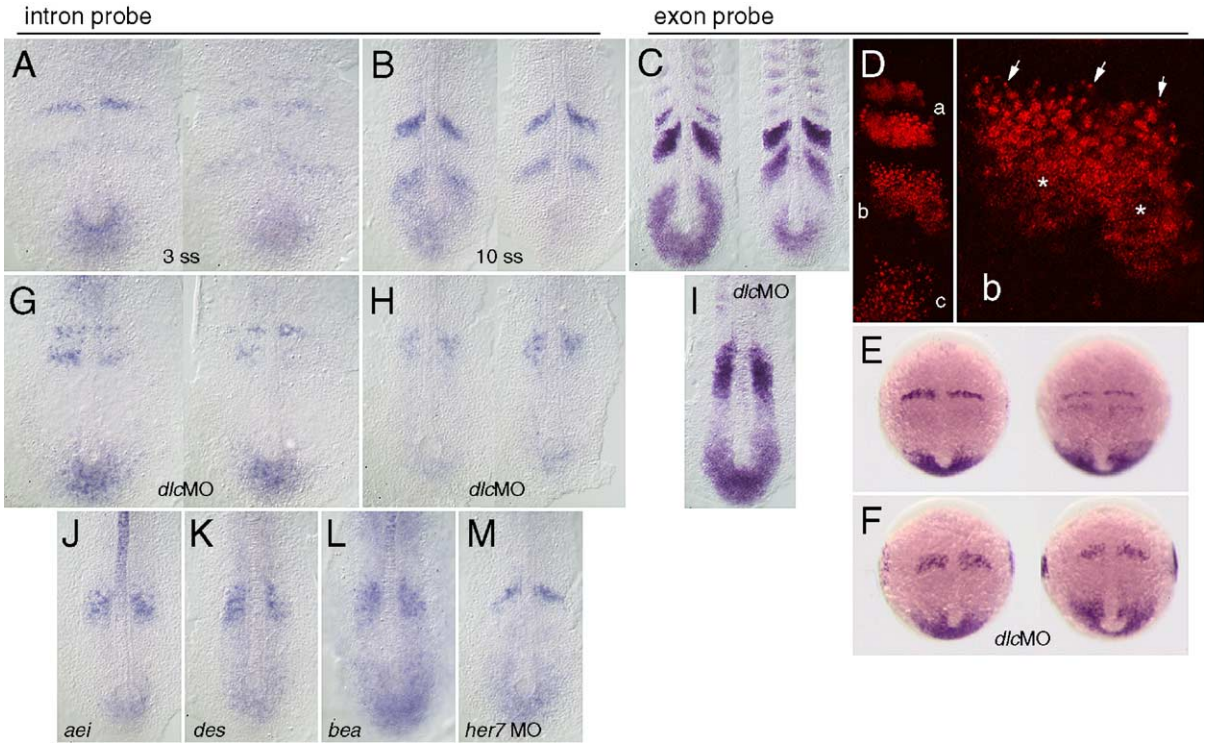

Fig. 4. Transcriptional activity of the *deltaC* gene in wild type and segmentation defective mutant backgrounds. Distribution of total *dlc* mRNA, detected with a cDNA-derived riboprobe, is shown in panels (C–F) and (I). Distribution of unspliced *dlc* pre-mRNA, detected with a riboprobe to the fourth intron, is shown in panels (A), (B), (G), (H), and (J–M). Dorsal view in flat mounted embryos in wild type (A–E), morpholino injected (F–I.M), and mutant (J, *aei/dld*; K *des/n1a*,; L, *bea*) backgrounds. Embryos are shown at bud (E, F), 3 (A, G), 7 (D), and 10 somite (B, C, H, I, J–M) stages of development. Panels (F–I) show the effect of injection of 1 ng/nL *dlc*MO3 and 2 ng/nL *dlc*MO4, and panel (M) shows the effect of 2 ng/nL *her7*MO1 and *her7*MO2. The total distribution of *dlc* mRNA in a representative embryo, as detected with the exonic riboprobe by confocal LSM, is shown in panel D, with (a) anterior, (b) mid-, and (c) posterior wavelike expression domains, (b) and is magnified in right panel showing puncta (arrows) on the rostral side, and diffuse staining (asterisks) in the caudal part of the expression domain.

in *dlc*MO-injected embryos. At bud stage, *dlc* showed variability in the extent of posterior expression around the tail bud and in the thickness of a diffuse stripe in the anterior PSM, suggesting some spatial coordination of cyclic expression remained (n = 13, Fig. 4E), similar to the *her* genes. At the 10 somite stage *dlc*MO-injected embryos were indistinguishable from each other, suggesting that cyclic expression was no longer coordinated (n = 15, Fig. 4I). At neither stage did the expression levels of *dlc* appear to be significantly decreased by *dlc*MOs; however, it is possible that *dlc* transcription was reduced but masked by MO-dependent stabilization of endogenous *dlc* mRNA, as has been observed for the cyclic *her* genes (Gajewski et al., 2003; Oates and Ho, 2002).

In 3 somite stage embryos injected with *dlc*MOs and assayed with the intron probe, multiple stripes were evident in the anterior PSM (n = 28, Fig. 4G), indicating that the single diffuse stripe seen with the exonic riboprobe in the anterior PSM after this treatment (Fig. 4F) concealed an underlying striped pattern of transcriptional activation. At the 10 somite stage, the *dlc* intron riboprobe revealed a single anterior domain of salt-and-pepper like expression

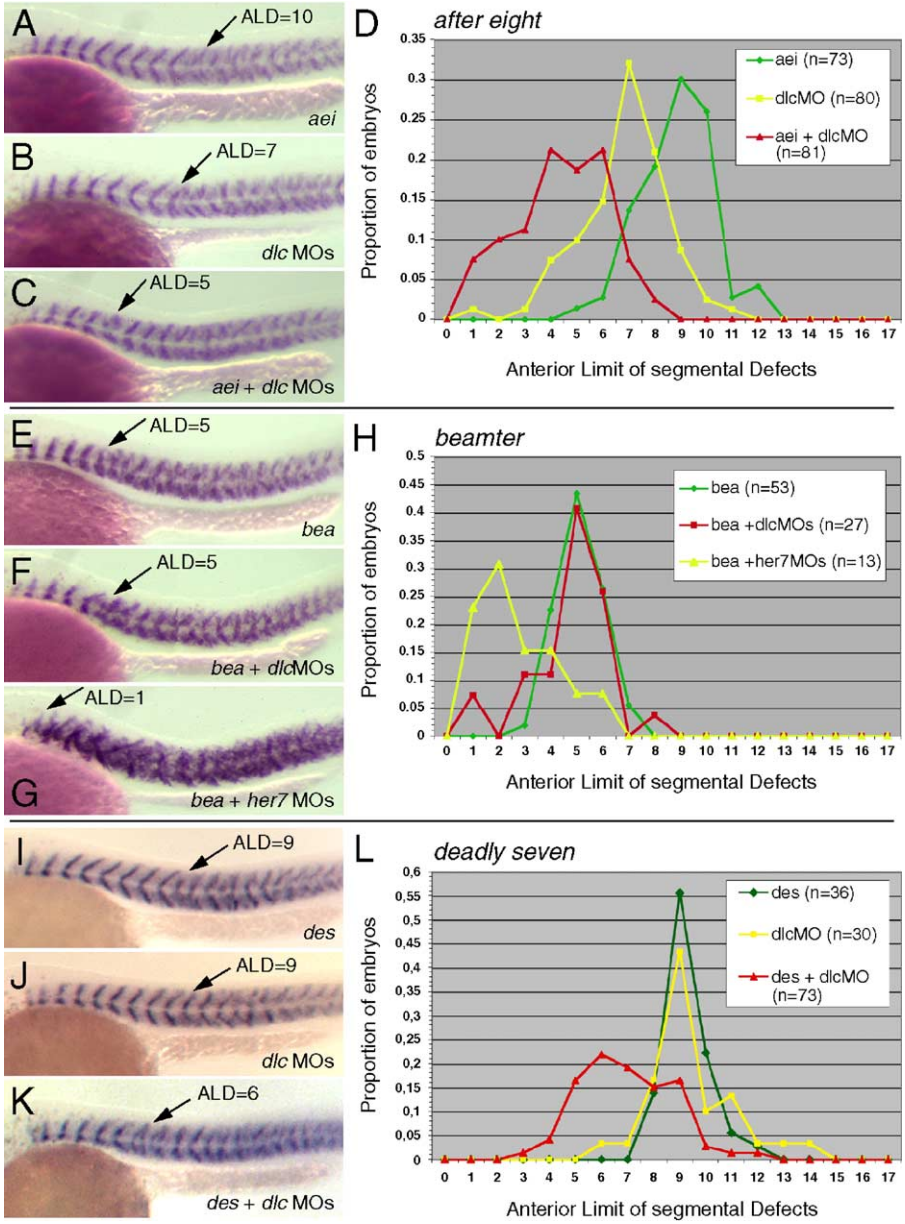

Fig. 5. Analysis of the interaction between *deltaC* and the *after eight/deltaD* (*aei/dld*), *beamter* (*bea*), and *deadly seven/notch1a* (*des/n1a*) mutations in the Delta/Notch signaling pathway. Myotome boundaries in the trunk are shown in 26 hpf embryos in lateral view with anterior to the left and dorsal upwards (A–C, E–G, I–K). (A) *aei/dld* uninjected, (B) wild type injected with 1 ng/nL *dlc*MO3 and 1 ng/nL *dlc*MO4, (C) *aei/dld* injected with *dlc*MOs. (E) *bea* uninjected, (F) *bea* injected with 1 ng/nL *dlc*MO3 and 2 ng/nL *dlc*MO4, (G) *bea* injected with 3 ng/nL *her7*MO1 and 3 ng/nL *her7*MO2. (I) *des/n1a* uninjected, (J) wild type injected with 0.5 ng/nL *dlc*MO3 and 0.5 ng/nL *dlc*MO4. (D, H, L) Histograms comparing Anterior Limit of Defects (ALD) for these nine conditions. Arrows in panel (A–C), (E–G), and (I–K) indicate ALD in each embryo.

(n = 24, Fig. 4H), in agreement with the exonic probe (Fig. 4I). However, in contrast to the exonic probe, the level of *dlc* transcript detectable in the tailbud and posterior PSM appeared reduced relative to the anterior domain, suggesting that stabilization of the endogenous mRNA by the morpholino was responsible for the high posterior expression observed with the exonic probe. Thus, in the posterior, cyclic expression region, reduction of *dlc* mRNA translation affects the level and pattern of activity of the transcription of the *dlc* gene itself, whereas in the anterior region where the cyclic domains have normally arrested, the patterning aspect appears to be primarily affected.

We also examined *dlc* pre-mRNA levels in Delta/Notch segmentation mutants *bea*, *aei/dld*, *des/n1a*, and in embryos injected with *her7*-targeted morpholinos (Oates and Ho, 2002, and see Fig. 6O for comparison). The pattern generated by the *dlc* intron probe was similar to that of the exon probe, however, the intron-derived probe showed a reduction in expression levels in posterior PSM and tailbud relative to the anterior domain (Figs. 4J–M), similar to that seen in the *dlc* morpholino experiments above (Figs. 4H,I). Two notable differences in pattern between the probes are the elevated expression levels in the notochord of *bea*, and particularly *aei/dld* mutants, seen with the intron probe (Figs. 4J,L), and the cryptic stripes seen in anterior PSM of the *des/n1a* mutant (Fig. 4K) and *her7*-morpholino treated (Fig. 4M) embryos, where a more solid domain of salt-and-pepper expression is seen with the exon probe (compare to right hand panels of Figs. 6K,N of Oates and Ho, 2002). Thus, these data indicate that the *dlc* exon probe has systematically over-estimated the number of cells actively transcribing the *dlc* gene in the PSM and revealed that that patterned transcriptional events may be concealed by extended mRNA persistence.

Interaction between deltaC and Delta/Notch signaling mutants after eight/deltaD, beamter, and deadly seven/notch1a

Restriction of segmentation defects to the posterior trunk and tail in embryos with a reduction of *dlc* function may be due to a distinct posterior role for the *dlc* gene in segmentation, or it may be due to a redundancy in function between *dlc* and other members of the segmentation oscillator, as was previously found for *her7* (Oates and Ho, 2002). To test these possibilities, we examined the onset of segmental defects in *aei/dld*, *bea*, and *des/n1a* embryos injected with *dlc*MOs. We observed a moderate rostral shift in the ALD of both *aei/dld* (Figs. 5A–D) and *des/n1a* mutant embryos (Figs. 5I–L) upon injection of low concentration *dlc*MOs indicating that *aei/dld* and *des/n1a* have some redundant functions in the trunk between segments 5 and 9 that are normally compensated for by *dlc*. Injection of higher concentrations of *dlc*MOs into *aei/dld* embryos resulted in a highly penetrant defect in yolk extension shape and tail outgrowth (data not shown), suggesting a redundant role for Delta signaling in tail formation, consistent with studies in *Xenopus* embryos (Beck and Slack, 2002), but detailed examination of this phenotype is beyond the scope of this report. Higher concentrations of *dlc*MOs in the *des/n1a* background did not show a shift of ALD into the very anterior trunk (data not shown), nor did high concentration *dlc*MOs in *bea* mutants (Figs. 5E,F,H), although injection of *her7*MOs in parallel experiments shifted the ALD in a *bea* background rostrally to the anterior end of the paraxial mesoderm as previously reported (Figs. 5G,H; Oates and Ho, 2002). The expression of *her1*, *her7*, and *dlc* was examined in all *dlc*MO-injected mutant embryos at the 10 somite stage, but no large difference in pattern was observed in the different backgrounds (data not shown). Together, these genetic interactions demonstrate redundancy between *dlc* and other Delta/Notch components in the formation of posterior segments and suggest that cooperative interactions within this group of genes are not involved in anterior segmentation.

Interaction between deltaC and her7 produces anterior segmental defects

We next addressed the possibility of interaction between *dlc* and *her7* in anterior segment formation. However, given the synergistic effects of using two *dlc*-targeted MOs, we first re-evaluated the *her7* knock down effect utilizing both *her7*-targeted MOs (Table 2). We found that the ALD

Fig. 6. Analysis of the interaction between *deltaC* and *her7*. Myotome boundaries in the trunk are shown in 26 hpf embryos in lateral view with anterior to the left and dorsal upwards (A, B). (A) Wild type, uninjected control, (B) injected with 3 ng/nL *her7*MO1 and 3 ng/nL *her7*MO2. (C) Histogram comparing ALD in populations of embryos injected with increasing amounts of combined *her7*MOs, where the two numbers (e.g. 1 + 1) in inset legend are the concentration of *her7*MO1 and *her7*MO2 morpholino, respectively in ng/nL. Embryos injected with doses higher than 3 + 3 of combined morpholinos exhibited necrosis and non-specific defects. (D) Wild type embryo injected with 2 ng/nL *her7*MO1 and 2 ng/nL *her7*MO2, (E) embryo injected with 1 ng/nL *dlc*MO3 and 2 ng/nL *dlc*MO4, (F) embryo injected with *her7*- and *dlc*MOs combined. Arrows in panels (A), (B), and (D–F) indicate Anterior Limit of Defects (ALD) in these embryos. (G) Histogram comparing ALD in populations of embryos injected with the treatments in panels (D–F). (H–O) Expression of the *her1* cyclic gene after injection of *dlc*- and *her7*MOs. Presomitic mesoderm of embryos at 80% epiboly (H, J) and bud (I, K) in whole mount. Comparison of coherent wavelike expression domains of *her1* expression in wild type (H, I) and *her7*- and *dlc*MO-injected embryos (J, K). In each panel (H, I), two wild type embryos with representative phases of cyclic gene expression patterns are shown. In contrast, *her7*- and *dlc*MO-injected embryos are indistinguishable from each other (J, K). (L–O) Expression of the cyclic gene *her1* in the PSM of embryos at 14 hpf (10 somites) in dorsal view after flat mounting with anterior up. (L) Two representative phases of cyclic *her1* expression in wild type, control embryo; (M) comparison of levels and patterns of *her1* expression after injection of *dlc*MOs (1 ng/nL *dlc*MO3 and 2 ng/nL *dlc*MO4), (N) *dlc*- and *her7*MOs at the concentrations mentioned, (O) *her7*MOs (2 ng/nL *her7*MO1 and 2 ng/nL *her7*MO2). For the treatments shown in panels (M–O), embryos in a batch were indistinguishable from each other.

shifted rostrally as *her7*MO dose increased but that it stabilized at an ALD of 10 (Figs. 6A–C), in agreement with our previous results and those of others (Henry et al., 2002; Oates and Ho, 2002). Upon co-injection of both *dlc*MOs and both *her7*MOs, we observed that the ALD of the resulting embryos was strongly shifted in a rostral direction

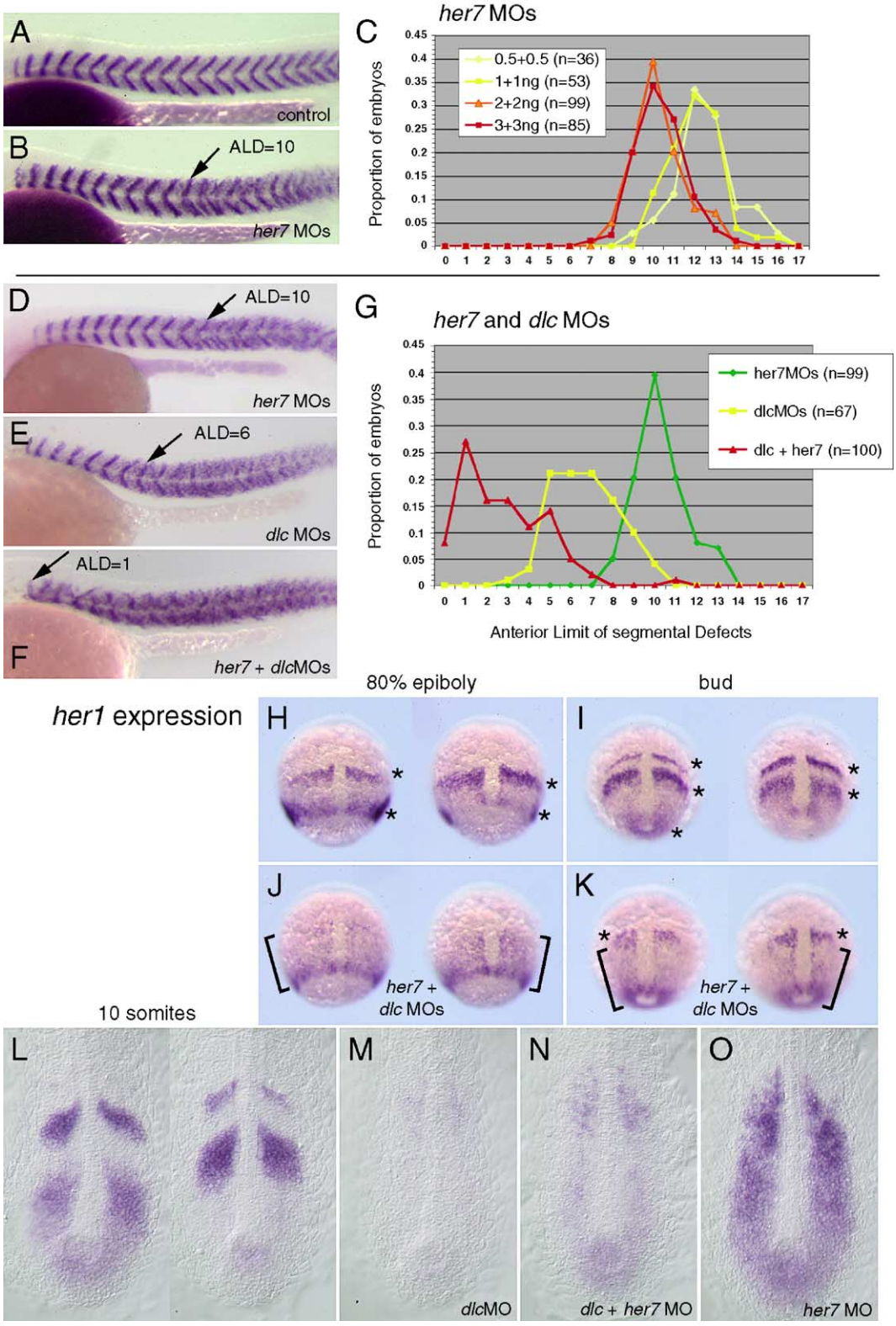

to the anterior end of the paraxial mesoderm (Figs. 6D–G), producing embryos that closely resembled those resulting from reduction of *her7* and *her1* functions (Henry et al., 2002; Oates and Ho, 2002). These results clearly demonstrate that *dlc* is required for the segmentation of the anterior trunk in combination with *her7*, indicating that the process is not controlled exclusively by the *her* genes.

The expression of markers of segment polarity in the PSM was examined at the 10 somite stage in embryos co-injected with *dlc*MOs and *her7*MOs. The expression of *myoD* (n = 33), *mespa* (n = 14), *mespb* (n = 15), *notch5* (n = 13), *papc* (n = 10), *fgf8* (n = 10), *dld* (n = 15), and *notch1a* (n = 8) was not significantly different from that observed after the injection of *dlc*MOs alone (data not shown), indicating that *dlc* is largely epistatic to *her7* with respect to the generation of segment polarity in the zebrafish PSM.

Embryos with an *her7*MO-induced ALD of 10 show a complete disruption of cyclic gene expression between the 10 and 13 somite stage, but largely normal expression earlier at bud stage (Oates and Ho, 2002). The ALD of 1 in animals lacking *dlc* and *her7* function suggested that the wavelike expression domains of the cyclic genes should be disrupted from their onset. Therefore, the expression of *her1* was examined at 80% epiboly when cyclic gene expression first becomes organized into stripes (n = 91, Figs. 6H,J), immediately before formation of the first somite at bud stage (n = 87, Figs. 6I,K), and 10 somites (data not shown and Fig. 6N, below) in embryos injected with *her7* and *dlc*MOs as above. In contrast to the wild type pattern, the injected embryos never developed coherent wavelike expression domains (Figs. 6J,K). Thus, complete disruption of cyclic expression domains correlates well with ALD, indicating that the loss of anterior segmentation in the *dlc* and *her7* combined knock down is due to a failure at the level of the oscillator genes.

Opposing effects of dlc and her7 on her1 expression levels

Finally, a comparison of the effect of reduction of *dlc* and *her7* function on the levels of cyclic gene expression was explicitly carried out by examining the expression of the cyclic *her1* gene in PSM of 10 somite embryos after injection of *dlc*MOs, or *her7*MOs, or a combination of both (Figs. 6L–O). The 10 somite time point was chosen because the PSM produces defective segments at this stage in both *dlc* and *her7*MO-injected embryos. Thus, the state of *her1* gene expression should reflect the end state of the defective segmentation oscillator in each of these reduction-of-function conditions. For these experiments, color development of the in situ was run in parallel on all treatments and allowed to proceed until the *dlc*MO-injected embryos first showed faint signal (approximately 30 min in our hands), then staining of all embryos was stopped. This was a considerably shorter development time than that used in Fig. 3, when the distribution of all *her1*-expressing cells was sought. In contrast to the alternating stripes of wild type cyclic expression domains seen in control embryos (Fig. 6L), injection of *dlc*MOs resulted in a dramatic decrease in *her1* expression levels throughout the PSM (n = 58, Fig. 6M). Injection of *her7*MOs had the opposite effect, causing widespread, high-level *her1* expression throughout the PSM (n = 70, Fig. 6O). Co-injection of both sets of MOs caused a weak expression of *her1* throughout the PSM that was intermediate between the individual treatments, although closer to the level of the *dlc* reduction-of-function (n = 28, Fig. 6N). Thus, in addition to roles in patterning the stripes, *dlc* is required for the maintenance of elevated levels of *her1* expression, whereas *her7* is required for the maintenance of *her1* gene repression.

Discussion

In this report, we have investigated whether Delta/Notch signaling is involved in the segmentation of the anterior trunk by testing pairwise interactions between the *deltaC* (*dlc*) cyclic gene and other components of the segmentation oscillator in zebrafish. We have shown that a reduced *dlc* function preferentially affects segmentation of the posterior trunk and tail, concomitant with a late failure of cyclic gene expression (Figs. 1, 3, 4), much like the *after eight*/*deltaD* (*aei*/*dld*) and *deadly seven*/*notch1a* (*des*/*n1a*) mutant phenotypes (Holley et al., 2000, 2002; Jiang et al., 2000; Oates and Ho, 2002; van Eeden, 1996). A combination of *dlc* knock down with either of these non-cyclic segmentation mutants shifts ALD rostrally (Fig. 5), indicating that there is redundancy between these genes in the segmentation of the posterior trunk. However, neither of these combinations, nor the *aei*/*dld*;*des*/*n1a* double affects the segmentation of the anterior-most 5 to 6 segments. Since these segments are also unaffected by knock down of the zebrafish *Su(H)* gene (Sieger et al., 2003), a critical mediator of Notch transcriptional target activation, these data are consistent with a role for Delta/Notch signaling confined to the patterning of the posterior segments.

A combined loss of the cyclic *her7* and *her1* genes causes segmental defects along the entire axis of the embryo (ALD = 1), concomitant with early disruption of cyclic gene expression (Henry et al., 2002; Oates and Ho, 2002), suggesting that the anterior trunk may be segmented by members of the *her* family of transcriptional repressor genes without the involvement of Delta/Notch signaling. However, we now show in this paper that a combined knock down of the *dlc* and *her7* genes, both of which have posterior ALDs in isolation, causes strong segmentation defects throughout the axis of the zebrafish embryo (ALD = 1) in a phenocopy of the combined *her1*;*her7* loss of function. Furthermore, these anterior defects are accompanied by a failure to initiate and maintain cyclic expression, indicating that they arise from a problem with the segmentation oscillator itself. Thus, the Delta family

member *dlc* has a role in anterior segmentation, strongly suggesting that the Delta/Notch pathway is required for the formation of anterior segments, as well as those in the posterior. Although these combined data do not exclude roles for other molecular pathways in somitogenesis, for example RPTPψ (Aerne and Ish-Horowicz, 2004), they are consistent with the hypothesis that a Her-based genetic oscillator is (1) tightly linked to the Delta/Notch signaling pathway, (2) used throughout somitogenesis, and (3) composed of elements that are redundant or parallel in function.

Previous analysis of delta and notch gene function in zebrafish segmentation: outputs or components of an oscillator?

Over-expression of mRNA encoding a dominant activating *notch1a* intracellular domain produces strong somitogenic defects in the zebrafish embryo, consistent with a role for Notch signaling in zebrafish segmentation (Takke and Campos-Ortega, 1999). In these animals, *her1* expression is diffuse in the PSM, although the relative level of expression is not commented upon, and *dlc* expression levels are reduced in the PSM and the striped pattern is lost. Furthermore, the somitogenic phenotype of *deadly seven* is caused by a mutation in *notch1a* (Holley et al., 2002) and in the PSM of this mutant the cyclic patterns of *her1*, *her7*, and *dlc* are lost, confirming a role for the *notch1a* gene in the generation of cyclic expression patterns (Holley et al., 2002; Jiang et al., 2000; Oates and Ho, 2002; van Eeden et al., 1998). Interestingly, the defective *dlc* expression patterns after gain or loss of Notch1a function are remarkably similar (Holley et al., 2002; Takke and Campos-Ortega, 1999), indicating that we cannot simply deduce whether Notch1a-mediated signaling activates or represses *dlc* expression. In contrast, the *her1* expression pattern distinguishes between these conditions and is consistent with an activating role for *notch1a*-mediated signaling in *her1* expression.

The over-expression of either *dlc* or *dld* (or a dominant negative form of *dld*) results in milder somitogenic defects than seen with an activated *notch1a* construct, but importantly, *her1* stripes were reported to be essentially normal in the PSM (Dornseifer et al., 1997; Takke and Campos-Ortega, 1999). These over-expression experiments suggested that some ligand(s) other than Dlc or Dld should be responsible for Notch1a activation in the PSM (Takke and Campos-Ortega, 1999). Thus, they imply that the zebrafish *dld* and *dlc* genes do not have a function in cyclic gene expression, that is, they are not components of the segmentation oscillator. In contrast, loss of function mutation of the non-cyclic *dld* gene (the *after eight* mutant, Holley et al., 2000) results in profound defects in the cyclic expression of *her1*, *dlc*, and *her7* in the PSM (Jiang et al., 2000; Oates and Ho, 2002; van Eeden et al., 1998), and in particular, a reduction of cyclic gene transcript in the intermediate and posterior PSM (current study and Oates and Ho, 2002). Furthermore, a previous morpholino-induced reduction of function of *dlc* resulted in a disruption of cyclic *her1* and *dlc* expression at the 10 somite stage (Holley et al., 2002), although the relative levels of expression were not measured. We now confirm that *dlc* function is required in the PSM for cyclic *her1* and *dlc* expression and further show that it is required for cyclic *her7* expression and cyclic transcription of the *dlc* gene itself. Moreover, in contrast to the over-expression experiments, *dlc* function can be distinguished from that of *dld* by its effect on the generation of segment polarity (see below). Combined, these loss of function experiments clearly implicate *dlc* as a component of the segmentation oscillator in the zebrafish, in agreement with the original hypothesis of Holley et al. (2002), and are consistent with both Dld and Dlc as endogenous ligands for the Notch1a receptor in this process. Nevertheless, several questions remain: since the combined *dlc* and *dld* loss of function phenotype reported here (ALD = 5) is more rostral than that of the *des/n1a* (ALD = 9), we predict that Notch1a is not the only receptor through which the Delta proteins can signal to generate the cyclic expression patterns. Furthermore, since the combined *dld* and *dlc* knock down does not affect the very anterior segments (ALD = 5), Dld and Dlc may not be the only DSL ligands active in the PSM. Alternatively, Dlc may act in the anterior trunk in a manner that does not require Notch activity, although Notch independent roles for Delta proteins are not currently known. Indirect support for this idea comes from Sieger et al. (2003), who have suggested that Notch signaling ought only be involved in posterior segmentation on the basis that MO-depletion of a zebrafish *Su(H)* leaves the first five segments intact. The existence of additional *Su(H)* genes or *Su(H)*-independent Notch signaling would compromise this hypothesis.

All known Notch-dependent cyclic genes are transcriptionally controlled

Dynamic cyclic expression patterns in the PSM could in principle be generated by ubiquitous transcription and regionally controlled mRNA breakdown. Cyclic transcriptional regulation of members of the Her and Lfng families has been established from promoter analysis of *her1* in zebrafish (Gajewski et al., 2003) and *Lfng* in mouse (Cole et al., 2002; Morales et al., 2002), and the use of intron probes to *her1* and *Lfng* in zebrafish and chick (Gajewski et al., 2003; Morales et al., 2002) and *Hes7* in mouse (Hirata et al., 2004). We have demonstrated that the distribution of *dlc* pre-mRNA mimics the pattern of mRNA (Fig. 4), indicating that the *dlc* cyclic expression patterns are also controlled at the transcriptional level. Thus, for every cyclic gene family examined, transcriptional activation is the mechanism used to generate the dynamic striped pattern of cyclic gene mRNA, arguing that transcriptional control is central to the oscillatory mechanism. In addition, we have examined the

structure of individual wavelike expression domains in the intermediate PSM and find that the sub-cellular distribution of *dlc* mRNA is not homogeneous across each stripe, with punctate distribution of signal on the rostral boundary of stripes, and a diffuse cellular signal in the caudal half. These observations are consistent with the activation of *dlc* transcription on the rostral edge of an anteriorly-traveling wavelike expression domain and subsequent persistence of mRNA in the absence of continued transcription in the caudal extent of each domain. The high predominance of punctate and nuclear staining in the posterior PSM and tailbud is consistent with a rapid cycle time in which cytoplasmic mRNA does not long accumulate, whereas the even distribution of cellular staining in stripes in the anterior PSM is consistent with the slowing and arrest of the cyclic expression domains in this tissue. Combined, these heterogeneous distributions provide independent evidence for the mobility and directionality of cyclic expression domains within the PSM.

Repressor versus activator functions of the components of the oscillator

Loss of function of *her1*, or *her7*, or a combination of *her1* and *her7* have all been reported to result in the loss of cyclic expression domains through widespread derepression of cyclic gene expression (Henry et al., 2002; Holley et al., 2002; Oates and Ho, 2002), only differing in how rapidly this state was achieved. Nevertheless, data from two studies indicate that some form of oscillatory behavior persists despite reduced *her1* function (Gajewski et al., 2003; Oates and Ho, 2002). Our finding that *dlc* is required for activation and maintenance of the expression levels of the cyclic genes contrasts its function with that of the *her* genes. Thus, among the cyclic genes, we have now identified distinct activating and repressing oscillator components in the zebrafish. These data are consistent with a model in which each cycle of gene expression is driven in distinct phases. In this view, the cyclic gene "on" phase, driven in part by *dlc* activity, is required to form the anterior boundary and the body of the wavelike expression domain, and the cyclic gene "off" phase, driven in part by *her7* activity, is required to form the anterior boundary and body of the interstripe. As reported in this paper, the role of *dlc* as an activator opposed to the *her* repressors therefore meets a prediction of our previously published model for Delta/Notch function within the segmentation oscillator (Fig. 10 in Oates and Ho, 2002). Nevertheless, we note that our observations (e.g. Figs. 6L–O) are made on the effects of gene loss of function accumulated over time and that direct activating or repressing activities within the period of one cycle have yet to be observed in any system.

Interestingly, *dlc* function in zebrafish appears to be the opposite of chick *Lfng*, which, upon over-expression, leads to the repression of the cyclic genes (Dale et al., 2003), suggesting that these two cyclic genes do not play analogous roles in the oscillator. In conclusion, our data are consistent with a modification of the original proposal by Jiang et al. (2000) that the function of cyclic *dlc*, and Delta/Notch signaling in general, is restricted to the synchronization of oscillations in neighboring cells. Our findings of a clear reduction in *her1* and *her7* expression levels as a result of reduced *dlc* function suggest that cyclic *dlc*, and Delta/Notch signaling in general, plays an additional role in the maintenance of the amplitude of the oscillations, as well as in their synchronization.

How does the oscillator affect segment polarity?

While all the Delta/Notch morpholinos and mutations examined to date cause defective segment polarity, the effects of loss of function of the cyclic *her7* and *dlc* genes are different, exemplified by their divergent action on *mespa* and *notch5* expression (Figs. 2E,G). In the case of *mespa*, *dlc* appears much closer in function to *aei/dld*, *des/n1a*, and *bea* in that *mespa* is not expressed at all than to *her7* where *mespa* stripes are strongly disorganized. Expression of *notch5* in the PSM depends critically on *dlc*, whereas in *aei*/*dld* embryos *notch5* is still expressed in a diffuse band in the anterior PSM, and in *her7* knock down embryos, *notch5* expression levels are unaffected, although disorganized like *mespa*. The absolute requirement for *dlc* function in the expression of *mespa* and *notch5* may provide an important avenue of inquiry into how the variable states of the oscillator are read out in terms of segment polarity. However, it is not yet clear whether the effect on the expression of the *mespa* and *notch5* segment polarity genes is a direct consequence of defective oscillator function, or whether it is caused by the lack of a later function for *dlc* in the anterior-most PSM. An example of a Delta/Notch gene with spatially separated functions in segmentation is found in the mouse where control of *Dll1* expression in the PSM and somites is separable by its dependency on *Presenilin1* function (Takahashi et al., 2000, 2003).

Time course of oscillator failure as an indicator of redundant structure

As first noticed by Jiang et al. (2000), mutant zebrafish embryos with a posterior ALD experience a gradual decay in the wavelike expression patterns of cyclic genes, with the important correlation that the more anterior the ALD, the more rapidly the wavelike expression domains decay. This observation was found to hold also for the cyclic *her7* reduction-of-function phenotypes (Oates and Ho, 2002), and we now show that the same effect underlies the cyclic *dlc* reduction-of-function phenotype. The relatively gradual decay of wavelike expression patterns prior to the sudden onset of segmentation defects means that apparently normal segmentation can occur in the presence of imperfect cyclic expression and implies that there must be a threshold relationship (a non-linearity) between the coherence of

Table 3
Anterior Limit of Defects (ALD) after reduction or loss of function of oscillator components

	Alone	*her7*MO	*dlc*MO
*her7*MO	10	–	1
aei	9	6	5[a]
des	9	6	6[a]
bea	5	1	5
*dlc*MO	5	1	–

[a] This interaction was measured at a concentration of *dlc*MO that did not, in isolation, give the ALD indicated in the "alone" column, therefore, it indicates interaction, but not necessarily the absolute anterior limit.

cyclic expression patterns and ability of the PSM to segment correctly. Generalizing this finding to segmentation in amniotes awaits careful studies in mutant mouse embryos relating somitic phenotype to changes in cyclic gene expression patterns throughout a developmental time series.

By varying the dose of *dlc* morpholinos, the ALD can be set at different positions along the axis, with higher doses giving more rostral ALDs (Fig. 1) up to an anterior limit of segment 5. The ability to select the position at which segmentation becomes defective by varying the level of translational inhibition of a target mRNA argues that the segmentation process is extremely sensitive to the level of protein. We predict that hypomorphic alleles of *aei*/*dld* and *des*/*n1a* will also show more posterior ALDs than those displayed by the characterized null alleles (Holley et al., 2000, 2002). By combining *her7* or *dlc* morpholino treatments with *aei/dld*, *des/n1a*, or *bea* mutations, the ALD can also be shifted rostrally without an obvious qualitative change in the severity of the myotomal segmental defects (Table 3). Furthermore, the severity of these defects does not appear to depend on whether an activator (*dlc*) or repressor (*her7*) of cyclic gene expression has been disrupted. With our methods, we have been unable to observe the alternating boundary defects reported by Henry et al. (2002). Thus, it appears as though the parameter that is being affected in these combination phenotypes is principally the *rate* at which the wavelike expression domains decohere to the point that segmentation is aberrant. Wavelike gene expression in *bea* mutants and *dlc* morphants decays at approximately the same rate, which is faster than *aei/dld* and *des/n1a* mutants, which is faster again than *her7* morphants. The slowest decay rates seen to date are for the knock down of *her4* and *her6*, where ALD was observed at segments 23 and 20, respectively (Pasini et al., 2004). The different decay rates caused by removing different components of the oscillator suggest that the quantitative contribution of each part to oscillator function is not equal. Adding two defects together speeds the rate of decay further: in *her7*;*dlc* double morphants, wavelike gene expression decays faster than either *her7* or *dlc* morphant, and in *her7*;*aei/dld* or *her7*;*des*/*n1a* morphant-mutant combinations decays faster than *her7*, *aei*/*dld*, or *des*/*n1a* morphant or mutant in isolation. Note that the decay rate is not correlated with whether the decoherent expression domains are maintained at low (e.g. *dlc* ALD = 5, *aei/dld* ALD = 9) or high levels (e.g. *her7* ALD = 10, *her1;her7* ALD = 1). Importantly, the strong shift in ALD to the very anterior end of the paraxial mesoderm is only seen with *her1*;*her7* and *dlc*;*her7* combinations; all other reported combinations appear to shift ALD by a small number of segments and to be restricted to the axial level of the *bea* or *dlc* phenotype. Why this should be the case is unclear. We propose that, in the absence of *her1* and *her7*, the system may be unable to generate any autonomous oscillations because it cannot repress cyclic expression at all, leading to early failure, whereas in the absence of *dlc* and *her7*, early failure may be the consequence of loss of activation and synchronization, as well as reduced capacity to repress. Quantitative measurements of mRNA and protein levels as well as direct measurement of oscillator frequency may be necessary to understand this system in full.

An exception to the additive nature of the phenotypes is the combination of loss of *dlc* in a *bea* genetic background, since in this case there is no rostral shift in ALD. The available indirect evidence strongly supports membership of *bea* in, or interaction with, the Delta/Notch signaling pathway (Durbin et al., 2000; Holley et al., 2000, 2002; Jiang et al., 2000; Oates and Ho, 2002; Sawada et al., 2000; van Eeden et al., 1996, 1998). The identical ALD (at segment 5) of single gene loss of function phenotypes of *bea* and *dlc*MOs, the failure to modify the *bea* ALD by injection of *dlc*MOs, and the identical combined knock down phenotype with *her7* raised the possibility that *bea* is a lesion in the *dlc* gene. Indeed, during the preparation of this manuscript, it was reported that *bea* maps to the *dlc* locus on Chr 15 (Scott Holley, Yun-Jin Jiang, personal communication), a finding that would be consistent with our analysis of the *dlc* morpholino-induced phenotype, and provide an explanation for our earlier results showing a strong interaction between *her7* and *bea* (Figs. 6C,F,J in Oates and Ho, 2002).

In summary, we have demonstrated a role for the cyclic *deltaC* gene, in cooperation with the *her7* cyclic gene, in the patterning and formation of anterior somites in zebrafish, indicating that the anterior is not patterned exclusively by a Her gene-based mechanism. This strongly suggests that Delta/Notch signaling is required for the correct segmentation of the paraxial mesoderm along the entire axis, although in a manner that is protected in the anterior by genetic redundancy. Thus, the segmentation oscillator appears to utilize the same components in the anterior and posterior trunk, although the robustness of the genetic interactions among them changes.

Acknowledgments

The authors wish to thank the Ho lab for discussions, Carl-Phillip Heisenberg, Laurel Rohde, Ashley Bruce, Karen Echeverri, Karla Neugebauer, Isaac Skromne, Dae-

Gwon Ahn, and Scott Holley for constructive criticism of various versions of the manuscript, and Devon Mann for excellent fish care and laboratory management. We also acknowledge the communications and ideas of Clarissa Henry, Yun-Jin Jiang, Scott Holley, Martin Gajewski, Alan Rawls, and everyone in the segmentation discussion group present at the June 2002 Zebrafish Genetics and Development conference in Madison, WI, USA. This research was funded by grants from the NIH and the March of Dimes.

References

Aerne, B., Ish-Horowicz, D., 2004. Receptor tyrosine phosphatase ψ is required for Delta/Notch signaling and cyclic gene expression in the presomitic mesoderm. Development 131, 3391–3399.

Aulehla, A., Johnson, R.L., 1999. Dynamic expression of lunatic fringe suggests a link between notch signaling and an autonomous cellular oscillator driving somite segmentation. Dev. Biol. 207, 49–61.

Aulehla, A., Wehrle, C., Brand-Saberi, B., Kemler, R., Gossler, A., Kanzler, B., Herrmann, B.G., 2003. Wnt3a plays a major role in the segmentation clock controlling somitogenesis. Dev. Cell 4, 395–406.

Barrantes, I.B., Elia, A.J., Wunsch, K., De Angelis, M.H., Mak, T.W., Rossant, J., Conlon, R.A., Gossler, A., de la Pompa, J.L., 1999. Interaction between Notch signalling and Lunatic fringe during somite boundary formation in the mouse. Curr. Biol. 9, 470–480.

Beck, C.W., Slack, J.M., 2002. Notch is required for outgrowth of the *Xenopus* tail bud. Int. J. Dev. Biol. 46, 255–258.

Bessho, Y., Miyoshi, G., Sakata, R., Kageyama, R., 2001a. Hes7: a bHLH-type repressor gene regulated by Notch and expressed in the presomitic mesoderm. Genes Cells 6, 175–185.

Bessho, Y., Sakata, R., Komatsu, S., Shiota, K., Yamada, S., Kageyama, R., 2001b. Dynamic expression and essential functions of Hes7 in somite segmentation. Genes Dev. 15, 2642–2647.

Bessho, Y., Hirata, H., Masamizu, Y., Kageyama, R., 2003. Periodic repression by the bHLH factor Hes7 is an essential mechanism for the somite segmentation clock. Genes Dev. 17, 1451–1456.

Cole, S.E., Levorse, J.M., Tilghman, S.M., Vogt, T.F., 2002. Clock regulatory elements control cyclic expression of Lunatic fringe during somitogenesis. Dev. Cell 3, 75–84.

Conlon, R.A., Reaume, A.G., Rossant, J., 1995. Notch1 is required for the coordinate segmentation of somites. Development 121, 1533–1545.

Cui, Z., Clark, K.J., Kaufman, C.D., Hackett, P.B., 2001. Inhibition of skiA and skiB gene expression ventralizes zebrafish embryos. Genesis 30, 149–153.

Dale, J.K., Maroto, M., Dequeant, M.L., Malapert, P., McGrew, M., Pourquie, O., 2003. Periodic notch inhibition by lunatic fringe underlies the chick segmentation clock. Nature 421, 275–278.

Dornseifer, P., Takke, C., Campos-Ortega, J.A., 1997. Overexpression of a zebrafish homologue of the *Drosophila* neurogenic gene Delta perturbs differentiation of primary neurons and somite development. Mech. Dev. 63, 159–171.

Dunwoodie, S.L., Clements, M., Sparrow, D.B., Sa, X., Conlon, R.A., Beddington, R.S., 2002. Axial skeletal defects caused by mutation in the spondylocostal dysplasia/pudgy gene Dll3 are associated with disruption of the segmentation clock within the presomitic mesoderm. Development 129, 1795–1806.

Durbin, L., Brennan, C., Shiomi, K., Cooke, J., Barrios, A., Shanmugalingam, S., Guthrie, B., Lindberg, R., Holder, N., 1998. Eph signaling is required for segmentation and differentiation of the somites. Genes Dev. 12, 3096–3109.

Durbin, L., Sordino, P., Barrios, A., Gering, M., Thisse, C., Thisse, B., Brennan, C., Green, A., Wilson, S., Holder, N., 2000. Anteroposterior patterning is required within segments for somite boundary formation in developing zebrafish. Development 127, 1703–1713.

Ekker, S.C., Larson, J.D., 2001. Morphant technology in model developmental systems. Genesis 30, 89–93.

Evrard, Y.A., Lun, Y., Aulehla, A., Gan, L., Johnson, R.L., 1998. Lunatic fringe is an essential mediator of somite segmentation and patterning. Nature 394, 377–381.

Gajewski, M., Sieger, D., Alt, B., Leve, C., Hans, S., Wolff, C., Rohr, K.B., Tautz, D., 2003. Anterior and posterior waves of cyclic her1 gene expression are differentially regulated in the presomitic mesoderm of zebrafish. Development 130, 4269–4278.

Henry, C.A., Urban, M.K., Dill, K.K., Merlie, J.P., Page, M.F., Kimmel, C.B., Amacher, S.L., 2002. Two linked hairy/Enhancer of split-related zebrafish genes, her1 and her7, function together to refine alternating somite boundaries. Development 129, 3693–3704.

Hirata, H., Yoshiura, S., Ohtsuka, T., Bessho, Y., Harada, T., Yoshikawa, K., Kageyama, R., 2002. Oscillatory expression of the bHLH factor Hes1 regulated by a negative feedback loop. Science 298, 840–843.

Hirata, H., Bessho, Y., Kokubu, H., Masamizu, Y., Yamada, S., Lewis, J., Kageyama, R., 2004. Instability of Hes7 protein is crucial for the somite segmentation clock. Nat. Genet. 750–754.

Holley, S.A., Geisler, R., Nusslein-Volhard, C., 2000. Control of her1 expression during zebrafish somitogenesis by a delta-dependent oscillator and an independent wave-front activity. Genes Dev. 14, 1678–1690.

Holley, S.A., Julich, D., Rauch, G.J., Geisler, R., Nusslein-Volhard, C., 2002. her1 and the notch pathway function within the oscillator mechanism that regulates zebrafish somitogenesis. Development 129, 1175–1183.

Hrabe de Angelis, M., McIntyre II, J., Gossler, A., 1997. Maintenance of somite borders in mice requires the Delta homologue DII1. Nature 386, 717–721.

Ishibashi, M., Ang, S.L., Shiota, K., Nakanishi, S., Kageyama, R., Guillemot, F., 1995. Targeted disruption of mammalian hairy and Enhancer of split homolog-1 (HES-1) leads to up-regulation of neural helix-loop-helix factors, premature neurogenesis, and severe neural tube defects. Genes Dev. 9, 3136–3148.

Itoh, M., Kim, C.H., Palardy, G., Oda, T., Jiang, Y.J., Maust, D., Yeo, S.Y., Lorick, K., Wright, G.J., Ariza-McNaughton, L., et al., 2003. Mind bomb is a ubiquitin ligase that is essential for efficient activation of Notch signaling by Delta. Dev. Cell 4, 67–82.

Jensen, J., Pedersen, E.E., Galante, P., Hald, J., Heller, R.S., Ishibashi, M., Kageyama, R., Guillemot, F., Serup, P., Madsen, O.D., 2000. Control of endodermal endocrine development by Hes-1. Nat. Genet. 24, 36–44.

Jiang, Y.J., Aerne, B.L., Smithers, L., Haddon, C., Ish-Horowicz, D., Lewis, J., 2000. Notch signalling and the synchronization of the somite segmentation clock. Nature 408, 475–479.

Jouve, C., Palmeirim, I., Henrique, D., Beckers, J., Gossler, A., Ish-Horowicz, D., Pourquie, O., 2000. Notch signalling is required for cyclic expression of the hairy-like gene HES1 in the presomitic mesoderm. Development 127, 1421–1429.

Kim, S.H., Jen, W.C., De Robertis, E.M., Kintner, C., 2000. The protocadherin PAPC establishes segmental boundaries during somitogenesis in *Xenopus* embryos. Curr. Biol. 10, 821–830.

Kimmel, C.B., Ballard, W.W., Kimmel, S.R., Ullmann, B., Schilling, T.F., 1995. Stages of embryonic development of the zebrafish. Dev. Dyn. 203, 253–310.

Koizumi, K., Nakajima, M., Yuasa, S., Saga, Y., Sakai, T., Kuriyama, T., Shirasawa, T., Koseki, H., 2001. The role of presenilin 1 during somite segmentation. Development 128, 1391–1402.

Kusumi, K., Sun, E.S., Kerrebrock, A.W., Bronson, R.T., Chi, D.C., Bulotsky, M.S., Spencer, J.B., Birren, B.W., Frankel, W.N., Lander, E.S., 1998. The mouse pudgy mutation disrupts Delta homologue Dll3 and initiation of early somite boundaries. Nat. Genet. 19, 274–278.

Leimeister, C., Dale, K., Fischer, A., Klamt, B., Hrabe de Angelis, M., Radtke, F., McGrew, M.J., Pourquie, O., Gessler, M., 2000. Oscillating expression of c-Hey2 in the presomitic mesoderm suggests that the

segmentation clock may use combinatorial signaling through multiple interacting bHLH factors. Dev. Biol. 227, 91–103.

Lewis, J., 2003. Autoinhibition with transcriptional delay: a simple mechanism for the zebrafish somitogenesis oscillator. Curr. Biol. 13, 1398–1408.

Li, Y., Fenger, U., Niehrs, C., Pollet, N., 2003. Cyclic expression of esr9 gene in *Xenopus* presomitic mesoderm. Differentiation 71, 83–89.

McGrew, M.J., Dale, J.K., Fraboulet, S., Pourquie, O., 1998. The lunatic fringe gene is a target of the molecular clock linked to somite segmentation in avian embryos. Curr. Biol. 8, 979–982.

Morales, A.V., Yasuda, Y., Ish-Horowicz, D., 2002. Periodic Lunatic fringe expression is controlled during segmentation by a cyclic transcriptional enhancer responsive to notch signaling. Dev. Cell 3, 63–74.

Muller, M., v Weizsacker, E., Campos-Ortega, J.A., 1996. Expression domains of a zebrafish homologue of the *Drosophila* pair-rule gene hairy correspond to primordia of alternating somites. Development 122, 2071–2078.

Nasevicius, A., Ekker, S.C., 2000. Effective targeted gene *knockdown* in zebrafish. Nat. Genet. 26, 216–220.

Oates, A.C., Ho, R.K., 2002. Hairy/E(spl)-related (Her) genes are central components of the segmentation oscillator and display redundancy with the Delta/Notch signaling pathway in the formation of anterior segmental boundaries in the zebrafish. Development 129, 2929–2946.

Oka, C., Nakano, T., Wakeham, A., de la Pompa, J.L., Mori, C., Sakai, T., Okazaki, S., Kawaichi, M., Shiota, K., Mak, T.W., et al., 1995. Disruption of the mouse RBP-J kappa gene results in early embryonic death. Development 121, 3291–3301.

Pasini, A., Jiang, Y.-J., Wilkinson, D.G., 2004. Two zebrafish Notch-dependent hairy/Enhancer-of-split-related genes, her6 and her4, are required to maintain the coordination of cyclic gene expression in the paraxial mesoderm. Development 131, 1529–1541.

Palmeirim, I., Henrique, D., Ish-Horowicz, D., Pourquie, O., 1997. Avian hairy gene expression identifies a molecular clock linked to vertebrate segmentation and somitogenesis. Cell 91, 639–648.

Pourquie, O., 2001. Vertebrate somitogenesis. Annu. Rev. Cell Dev. Biol. 17, 311–350.

Rhee, J., Takahashi, Y., Saga, Y., Wilson-Rawls, J., Rawls, A., 2003. The protocadherin papc is involved in the organization of the epithelium along the segmental border during mouse somitogenesis. Dev. Biol. 254, 248–261.

Rida, P.C.G., Minh, N.L., Jiang, Y.J., 2004. A notch feeling of segmentation and beyond. Dev. Biol. 265, 2–22.

Sawada, A., Fritz, A., Jiang, Y., Yamamoto, A., Yamasu, K., Kuroiwa, A., Saga, Y., Takeda, H., 2000. Zebrafish Mesp family genes, mesp-a and mesp-b are segmentally expressed in the presomitic mesoderm, and Mesp-b confers the anterior identity to the developing somites. Development 127, 1691–1702.

Sieger, D., Tautz, D., Gajewski, M., 2003. The role of Suppressor of Hairless in Notch mediated signalling during zebrafish somitogenesis. Mech. Dev. 120, 1083–1094.

Takahashi, Y., Koizumi, K., Takagi, A., Kitajima, S., Inoue, T., Koseki, H., Saga, Y., 2000. Mesp2 initiates somite segmentation through the Notch signalling pathway. Nat. Genet. 25, 390–396.

Takahashi, Y., Inoue, T., Gossler, A., Saga, Y., 2003. Feedback loops comprising Dll1, Dll3 and Mesp2, and differential involvement of Psen1 are essential for rostrocaudal patterning of somites. Development 130, 4259–4268.

Takke, C., Campos-Ortega, J.A., 1999. her1, a zebrafish pair-rule like gene, acts downstream of notch signalling to control somite development. Development 126, 3005–3014.

Thisse, B., Thisse, C., Weston, J.A., 1995. Novel FGF receptor (Z-FGFR4) is dynamically expressed in mesoderm and neurectoderm during early zebrafish embryogenesis. Dev. Dyn. 203, 377–391.

van Eeden, F.J., Granato, M., Schach, U., Brand, M., Furutani-Seiki, M., Haffter, P., Hammerschmidt, M., Heisenberg, C.P., Jiang, Y.J., Kane, D.A., Kelsh, R.N., Mullins, M.C., Odenthal, J., Warga, R.M., Allende, M.L., Weinberg, E.S., Nusslein-Volhard, C., 1996. Mutations affecting somite formation and patterning in the zebrafish, *Danio rerio*. Development 123, 153–164.

van Eeden, F.J., Holley, S.A., Haffter, P., Nusslein-Volhard, C., 1998. Zebrafish segmentation and pair-rule patterning. Dev. Genet. 23, 65–76.

Weinberg, E.S., Allende, M.L., Kelly, C.S., Abdelhamid, A., Murakami, T., Andermann, P., Doerre, O.G., Grunwald, D.J., Riggleman, B., 1996. Developmental regulation of zebrafish MyoD in wild-type, no tail and spadetail embryos. Development 122, 271–280.

Westin, J., Lardelli, M., 1997. Three novel Notch genes in zebrafish: implications for vertebrate Notch gene evolution and function. Dev. Genes Evol. 207, 51–63.

Yamamoto, A., Amacher, S.L., Kim, S.H., Geissert, D., Kimmel, C.B., De Robertis, E.M., 1998. Zebrafish paraxial protocadherin is a downstream target of spadetail involved in morphogenesis of gastrula mesoderm. Development 125, 3389–3397.

Zhang, N., Gridley, T., 1998. Defects in somite formation in lunatic fringe-deficient mice. Nature 394, 374–377.